PROCEEDINGS OF SCIENCE

The search for charged lepton flavor violation in the MEG & MEG II experiments

Francesco Tenchini[∗†]
INFN Pisa, Largo Bruno Pontecorvo 3, 56127 Pisa, Italy
E-mail: francesco.tenchini@pi.infn.it

Within the scope of the Standard Model, the $\mu^+ \to e^+\gamma$ decay is forbidden by lepton flavor conservation. Several lepton flavor violating extensions of the Standard Model however predict a measurable $\mu^+ \to e^+\gamma$ branching ratio. The MEG experiment at PSI presently holds the current best experimental limit for this decay (5.7×10^{-13} at 90% C.L.) and is currently being upgraded for an improvement of a factor 10 in sensitivity in a time scale of about 4 years. The MEG II upgrade R&D status will be presented, along with the current state of the MEG I data analysis.

16th International Workshop on Neutrino Factories and Future Neutrino Beam Facilities
25 -30 August, 2014
University of Glasgow, United Kingdom

[∗]Speaker.
[†]On behalf of the MEG collaboration.

1. Introduction to Lepton Flavor Violation

The Standard Model (SM) is built with the assumption of lepton flavor conservation and vanishing neutrino masses. This is however accidental, as lepton flavor is not associated to any explicit gauge symmetry. Recent observation of neutrino oscillations [1, 2, 3, 4] showed that flavor is indeed violated for neutral leptons and neutrinos have mass. This introduces the possibility of Lepton Flavor Violating (LFV) processes arising in the charged sector from loop contributions; however the branching ratio (BR) for such decays would be immeasurably small ($< 10^{-50}$). On the other hand, the majority of Beyond SM (BSM) theories (see for example [5, 6, 7]) naturally incorporate massive neutrinos and simultaneously predict LFV decays, such as $\mu^+ \to e^+\gamma$, at a measurable BR. Observation of such a decay would then constitute clear evidence of BSM physics, while improving the BR upper limits (UL) places strong constraints on the parameter space of new theories.

2. Signal and Background

The $\mu^+ \to e^+\gamma$ signature for positive muons decaying at rest is the simultaneous emission of a positron and photon pair in back-to-back directions. Both particles carry the same kinetic energy, $E_{e^+} = E_\gamma = m_{\mu^+}/2 = 52.8$ MeV; the positron mass is negligible. This signature, while very simple, can be reproduced by two background types:

1. The physical background originating from the radiative muon decay (RMD) at rest, $\mu^+ \to e^+\nu_e\bar{\nu_\mu}\gamma$.
2. The accidental (ACC) background, arising from the coincidence of positrons from the $\mu^+ \to e^+\nu_e\bar{\nu_\mu}$ (Michel) decay and photons from $e^+ - e^-$ annihilation in flight, RMD or bremsstrahlung inside the analysis window. This is the dominant background contribution.

3. The MEG Detector

The MEG experiment ([8], see Fig. 2) uses the πE5 muon beamline at PSI (Paul Scherrer Institut) to deliver a continuous beam of 3×10^7 μ^+/s to a thin 205 μm polyethylene stopping target[1]. The positron is tracked by a magnetic spectrometer, while a Liquid Xenon (LXe) detector measures the photon energy, time and position.

The MEG positron spectrometer consists in a set of 16 drift chambers (DC), each composed of two staggered layers of sense wires and cathodic foils, immersed in a gradient magnetic field. The positron timing is measured by a Timing Counter (TC) comprising two arrays of scintillating bars positioned at each end of the tracking volume. The magnetic field, produced by a superconducting solenoid (COnstant Bending RAdius, COBRA), is designed to quickly sweep out positrons emitted at high transverse momentum and provide a bending radius independent from the emission angle.

The photon detector is composed of a single volume ($\approx 800\ \ell$) of LXe, chosen as a scintillating medium for its uniformity, short decay time ($\tau \approx 45$ ns for photons and ≈ 22 ns for α) and large light yield ($\sim 40000\ \gamma$/MeV, comparable to inorganic scintillators). It is surrounded by

[1] Although up to 10^8 μ^+/s is possible, a lower rate is used to keep the ACC background under control.

846 Hamamatsu 2″ PMT, developed for low temperature operation and detection of VUV ($\lambda = 178$ nm) scintillation light.

The detector is continuously monitored by multiple calibration systems, among which are a Cockroft-Walton accelerator, an array of α sources mounted inside the LXe detector, 55 and 83 MeV γ from the charge-exchange reaction $\pi^- \mathrm{p} \to \pi^0 \mathrm{n}$, a neutron generator and a monochromatic positron beam. The combined use of these calibration sources guarantees optimized performance and detector stability over time.

4. Data Analysis

Analysis of MEG data, characterized by five kinematic observables ($E_\gamma, E_e, t_{e\gamma}, \theta_{e\gamma}$ *and* $\phi_{e\gamma}$) is performed as a combination of blind and likelihood methods. Events belonging to the window corresponding to $48 < E_\gamma < 58$ MeV and $|t_{e\gamma}| < 1$ ns (the "blinding box", BB) are hidden until the Probability Density Functions (PDFs) for the likelihood function are finalized. Data outside the BB, belonging to the so-called "sidebands", is used to optimize the analysis, study the ACC background and extract the corresponding PDF. Meanwhile the PDFs for signal (SIG) events and RMD background is obtained from measured experimental resolutions and calibration data. Different resolutions and correlations between observables are taken into account on a per-event basis. As a cross-check, a separate analysis using constant PDFs is used, offering consistent results.

The number of SIG, ACC and RMD events is then extracted simultaneously, by performing a maximum likelihood fit (see Fig. 1) to the distribution of the five observables in the analysis region of the BB, defined as $48 < \mathrm{E}_\gamma < 58$ MeV, $50 < \mathrm{E}_\mathrm{e} < 56$ MeV, $|\mathrm{t}_{\mathrm{e}\gamma}| < 0.7$ ns, $|\theta_{\mathrm{e}\gamma}| < 50$ mrad and $|\phi_{\mathrm{e}\gamma}| < 50$ mrad. The 90% C.L. upper limit on the number of SIG events is calculated through a frequentist method with a profile likelihood-ratio ordering [9], with the number of RMD and ACC events treated as a nuisance parameter. The upper limit on SIG is translated into an upper limit for $\mathrm{BR}(\mu^+ \to \mathrm{e}^+\gamma)$ using a normalization factor extracted from Michel decay events.

The analysis procedure was applied to the accumulated statistics from the 2009-2011 data taking period [10]. The analysis of the combined data gives an upper limit for $\mathrm{BR}(\mu^+ \to \mathrm{e}^+\gamma)$ of 5.7×10^{-13} at 90% C.L., currently the most stringent limit on the BR for this decay and an improvement of a factor of ~ 20 compared to the results of previous experiments [11].

The sensitivity of the experiment under a null signal hypothesis is estimated by taking the median of the distribution of the upper limits on the branching ratio obtained over a series of MC pseudo-experiments. The rates of RMD and ACC events used in the simulation are taken from experimental data in the sidebands. The resulting branching ratio sensitivity at 90% C.L. is 7.7×10^{-13}, which is found to be consistent with separate estimates obtained from likelihood fits outside the analysis region.

Data taking for MEG ended in 2013; the inclusion of data from the 2012-2013 will double the accumulated statistics. Several improvements will also be included, such as an algorithm to identify γ originating from positron annihilation in flight and a more accurate measurement of the magnetic field. The expected final sensitivity is of $\sim 5 \times 10^{-13}$.

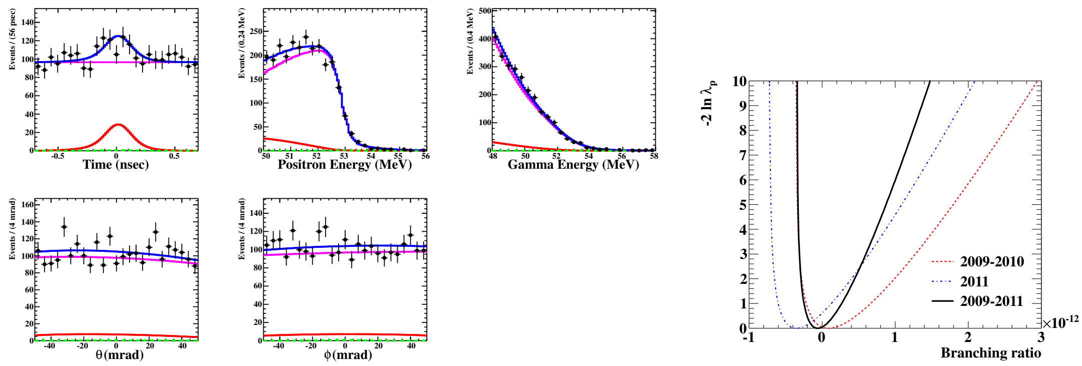

Figure 1: Left: Maximum Likelihood fit for the 2009-2011 data set. The color curves correspond to ACC (purple), RMD (red), SIG (dashed green) and combined (blue) likelihood functions. Right: Profile likelihood ratios as a function of BR for 2009-2010 data, 2011 data and the combined 2009-2011 data set.

5. MEG II Upgrade Plans

The current results already pose strong constraints on the parameter space for BSM theories. Further improvements however are currently limited by the contribution of accidental background, and thus by experimental resolutions. Given the large interest in the topic, the MEG collaboration has proposed an upgrade (MEG II) to the experiment, with the intent to improve the sensitivity by an additional order of magnitude [12]. The upgrade will be executed on a limited time scale, taking advantage of existing equipment where possible, in order to be competitive with next generation LFV experiments while maintaining a low cost.

The upgrade, an outline of which is shown in Fig. 2, affects all subdetectors.

The thickness of the target will be reduced from 205 μm to 140 μm, in order to minimize the material traversed by decay products before detection.

The positron tracker will be replaced by a single volume 190 cm long drift chamber using a stereo wire configuration, operating in a 85/15 mixture of Helium and Isobutane. This new detector will be more transparent, minimizing mutiple scattering while providing improved granularity and resolutions. A single hit resolution of 120 μm has been confirmed on small scale prototypes, which translates into a longitudinal resolution of ≈ 700 μm thanks to the stereo geometry. The angular resolution will improve from $8.7(\phi)/9.4(\theta)$ mrad to $\sim 4(\phi)/5(\theta)$ mrad, with a momentum resolution of 130 keV instead of the current 300 keV.

Multiple aging tests have been performed to check viability for high rate operation and a single cell full scale prototype has been built to verify mechanical feasibility. All tests have been successful.

The extended length of the chamber will allow better reconstruction of the particle trajectory up to the new Timing Counter system [13, 14], improving the tracking efficiency from 40% to 88%. The TC scintillator arrays will be replaced by two sets of 256 scintillator tiles, each read by Silicon PhotoMultipliers (SiPM). Thanks to the high time resolution of individual tiles and the use of combined information from multiple tile hits, the current timing resolution of 100 ps will be improved to ≈ 30 ps, as confirmed by dedicated tests in beam facilities.

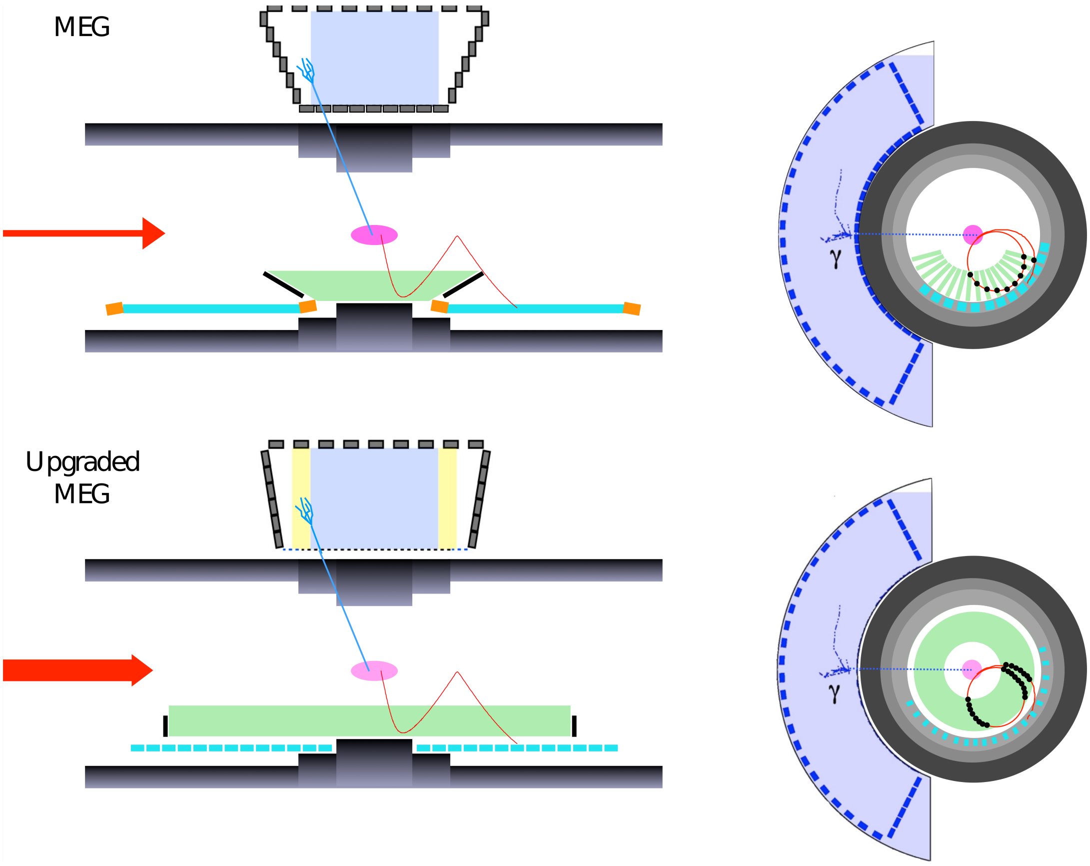

Figure 2: Overview of the present MEG experiment (above) and of the MEG II upgrade plan (below).

The LXe photon detector will be modified to provide a more uniform response. The orientation of PMTs in the lateral faces will be adjusted and the inner face widened to improve light collection at the edges. The inner face 2" PMTs will be replaced by a finer mesh of 12×12 mm^2 SiPM, leading to better and more uniform energy resolutions (1.0%, as opposed to the current 2.4% and 1.7% for shallow and deep events respectively) and position resolutions (~ 2 mm instead of the current 5 mm). The increased granularity will also improve pileup rejection, while the reduction of material on the photon trajectory will improve the detection efficiency from 63% to 70%.

In MEG, the waveforms from each detector are continuously digitized using the DRS chip developed at PSI [15]. In the upgrade scenario, the high bandwidth requirements of individual sub-detectors and the increased amount of channels require a redesign of the Data Acquisition (DAQ) Front-End. A new DAQ board based on the DRS chip is thus under development, allowing fast digitization at 2 GHz for DAQ and a separate 100 MHz sampling for trigger purposes.

Thanks to improved performances, it will be possible to raise the muon beam intensity to 7×10^7 μ^+/s, improving the statistics while keeping the ACC background under control.

The MEG II detector is currently under construction and an engineering run is expected to take place at the end of 2015, followed by three years of data taking starting in 2016. The sensitivity to the branching ratio of $\mu^+ \to e^+\gamma$ is expected to be $\sim 5 \times 10^{-14}$, a full order of magnitude more stringent than the current limit.

Acknowledgments

This work is partly supported by the Future in Research (FIRB) grant RBFR08XWGN, under the MIUR (Italian Ministry of University and Research) patrocine.

References

[1] K. Abe et al., *Indication of Electron Neutrino Appearance from an Accelerator-produced Off-axis Muon Neutrino Beam*, *Phys. Rev. Lett.* **107** (2011) 041801, [hep-ex/1106.2822].

[2] J. Ahn et al., *Observation of Reactor Electron Antineutrino Disappearance in the RENO Experiment*, *Phys. Rev. Lett.* **108** (2012) 191802 [hep-ex/1204.0626].

[3] F. An et al., *Observation of electron-antineutrino disappearance at Daya Bay*, *Phys. Rev. Lett.* **108** (2012) 171803 [hep-ex/1203.1669].

[4] Y. Abe et al., *First Measurement of θ_{13} from Delayed Neutron Capture on Hydrogen in the Double Chooz Experiment*, *Phys. Lett. B* **723** (2013) 66 [hep-ex/1301.2948].

[5] S. Antusch et al., *Impact of θ_{13} on lepton flavour violating processes within SUSY seesaw*, *JHEP* **11** (2006) 090 [hep-ph/0607263].

[6] L. Calibbi et al., *Flavour violation in supersymmetric SO(10) unification with a type II seesaw mechanism*, *JHEP* **0912** (2009) 057 [hep-ph/0910.0377].

[7] G. Blankenburg et al., *Neutrino Masses and LFV from Minimal Breaking of $U(3)^5$ and $U(2)^5$ flavor Symmetries*, *Eur. Phys. J. C* **72** (2012) 2126 [hep-ph/1204.0688].

[8] J. Adam et al., *The MEG detector for $\mu^+ \to e^+\gamma$ decay search*, *Eur. Phys. J. C* **73** (2013) 2365 [physics.ins-det/1303.2348].

[9] G. J. Feldman and R. D. Cousins, *A Unified approach to the classical statistical analysis of small signals*, *Phys. Rev. D* **57** (1998) 3873 [physics/9711021].

[10] J. Adam et al., *New constraint on the existence of the $\mu^+ \to e^+\gamma$ decay*, *Phys. Rev. Lett.* **110** (2013) 201801 [hep-ex/1303.0754].

[11] M. Ahmed et al., *Search for the lepton-family-number nonconserving decay $\mu^+ \to e^+\gamma$*, *Phys. Rev. D* **65** (2002) 112002 [hep-ex/0111030].

[12] A. Baldini et al., *MEG Upgrade Proposal*, physics.ins-det/1301.7225.

[13] M. De Gerone et al., *Design and test of an extremely high resolution Timing Counter for the MEG II experiment: preliminary results*, *JINST* **9** (2014) C02035 [physics.ins-det/1312.0871].

[14] P.W. Cattaneo et al., *Development of high precision timing counter based on plastic scintillator with SiPM readout*, *IEEE Trans.Nucl.Sci.* **61** (2014) 2657 [physics.ins-det/1402.1404].

[15] S. Ritt, R. Dinapoli and U. Hartmann, *Application of the DRS chip for fast waveform digitizing*, *Nucl. Instr. Meth. A* **623** (2010) 486.